A novel thermal anemometry technique for very-low-velocity flow measurement

Paul Nathan, Alan Robins and David M. Birch*

University of Surrey Centre for Aerodynamics and Environmental Flows, Guildford, Surrey GU2 7XH

E-mail: d.birch@surrey.ac.uk

Abstract

A novel thermal anemometry technique has been developed which uses CMOS sensor materials in order to enable a constant-temperature system to operate at overheat ratios significantly lower than conventional platinum-tungsten wires. Because of the low overheat ratios, the velocity induced by the buoyancy of the sensor's own thermal wake is minimized, and the sensor can be calibrated and used at speeds as low as 0.01 m/s. As a consequence, these sensors are suitable for use in atmospheric flow applications (either field anemometry or wind-tunnel models). The system was miniaturized and flush-mounted on the surfaces of wind-tunnel models approximating generic buildings, which were then placed in calibration flows at varying incidence angles. Results demonstrate that the surface-mounted thermal anemometry system may also be used to infer surface velocity distributions at low speeds over a model.

Introduction

Although the Reynolds numbers in the atmospheric boundary layer (and wind-tunnel approximations) tends to be very high, the dimensional flow speeds are not. This leads to significant difficulties in the measurement of these velocities, as many of the conventional air velocity measurement instruments available have minimum thresholds which are of the same order as the velocities of interest in atmospheric applications. Laser flow diagnostics, such as particle-image velocimetry and laser-Doppler anemometery, require flow seeding; in air, the density ratios of the seeding particles can exceed 10^3, resulting in significant particle tracking error (especially in highly vortical wakes: see, for example, Birch & Martin 2013). Pressure-based velocity measurement systems, such as Pitot or multi-hole probes, measure the dynamic pressure rise caused by the presence of the probe itself. Since the relationship between velocity and pressure is nonlinear, acceptable sensitivities at low speeds require pressure sensors with extremely small full-scale ranges or low uncertainty, and this technology is not always readily available. Conventional hot-wire probes are also problematic at very low speeds: in order to be sufficiently sensitive to changes in convective cooling, the temperature of the probe filament must be kept so high that the signal is dominated by the velocity induced by the sensor's own buoyant plume. LIDAR and ultrasonic systems offer some options for field measurements, but the high cost of these systems can preclude their use in large, distributed arrays.

There have been some efforts to improve the sensitivity dR_w/dT_w (where R_w is the total sensing element resistance and T_w the temperature of the sensing element) by replacing the traditional tungsten sensor wire with some semiconductor material for the purposes of measuring low velocity in air (see Mauconduit & Trinite 1976 and Fujita *et al.* 1995, for example). This enables the sensor system to work at much lower set temperatures, reducing the velocity induced by the thermal plume. These systems were effective, but were non-directional and fairly large. Ultra-miniature and application-specific IC thermal anemometers based on semiconductor and CMOS materials have also been developed (Mayer *et al*. 1997*a*, 1997*b*), although owing to the high failure rate, fragility and cost, these have not been widely adopted.

For the present study, a sub-millimetre block of CMOS NTC thermistor material has been used as a sensing element, together with signal conditioning and data acquisition hardware sufficiently miniaturized to be locally mounted, thereby eliminating noise and interference normally associated with the use of extended small-signal leads.

METHODOLOGY

The sensing element was driven in constant-temperature mode using a conventional Wheatstone bridge and power-amplifier arrangement (see Figure 1), although the configuration needed to be modified to suit the characteristics of a material having a negative temperature coefficient. The overheat ratio was fixed to ~1.2, so that the sensor would operate at ~60°C when used in standard room-temperature ambient conditions. A reference temperature sensor was co-located with the velocity sensor, in order to provide data for temperature corrections. The bridge driving voltage was then low-pass filtered and amplified, before being digitized using a custom 16-bit analogue-to-digital conversion system. All analogue and digital signal processing was carried out on the same printed circuit board, measuring not more than 13 mm × 46 mm. Digital signals were streamed from the system using an RS-485 protocol in order to facilitate networking.

The sensing element itself was a square cylinder measuring approx. 0.25 mm × 0.25 mm × 0.8 mm, and was precision-soldered onto the circuit card using 20 mm lengths of 200 μm-diameter hardened steel prongs. Care was taken to minimize the amount of solder used between the prongs and the sensor, to prevent error from conductive heat transfer, as well as to minimize prong wake effects. Because of the sensor element geometry, it was expected that the three-dimensional effects around the sensor itself would be significant and that the bandwidth of the system would be significantly lower than that of a conventional 5 μm-diameter tungsten hot-wire probe.

The bare sensing element was then calibrated, in order to establish its performance characteristics. The CTA system showed a reasonable sensitivity when the sensor was mounted with its long axis normal to the flow (see Figure 2), and responded to very low velocities: signals were obtained at speeds as low as 10 mm/s by towing the sensor system through air, although the process was insufficiently repeatable (owing to mechanical limitations of the towing apparatus) to calibrate the sensor at very low speeds.
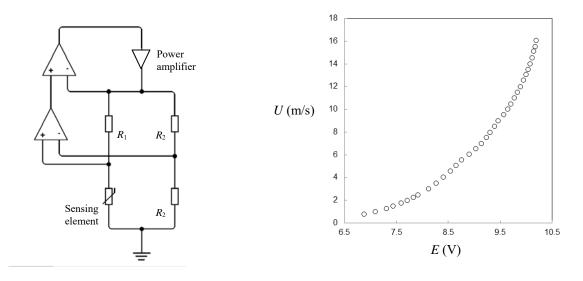

Figure 1: Schematic of the CTA control circuit   **Figure 2:** Calibration curve for bare sensor

The sensor systems were then mounted into nylon enclosures. The enclosures featured a flat, 10 mm-diameter reference surface through which the sensor prongs could project (via a 2 mm × 4 mm rectangular hole at its centre). The position of the sensor system within the enclosure could be adjusted such that the sensing element was just flush with the reference surface. The sensor was then cemented in place, and the hole sealed behind the sensor with non-conductive sealant. In this way, the sensing element was at the centre of a small sealed cavity. Arrays of sensor systems within these enclosures were then mounted internally in two idealized building models intended to demonstrate capability. The

first model was a hemisphere fitted with 13 sensors (one on the axis, six at 40° from the axis with equal azimuthal spacing, and six at 80° from the axis, spaced equidistantly). The second model was a circular cylinder capped with a hemisphere (such that the length of the cylinder was 1.33D, where D is the diameter), with five sensors located 0.1D below the junction between the cylinder and the hemisphere (see figure 3). Five sensors were selected, as this is the minimum number for which at least one sensor will be located in attached flow given any free-stream conditions. The models were intended to evaluate the surface velocity sensing system in idealized three- and two-dimensional configurations: the former for assessing local shear velocities near the surface, and the latter for assessing global incident velocity. The models were tested at Reynolds numbers Re_D of 4.5×10^3 to 7.2×10^4 in undisturbed free-stream flow at angles of incidence of at least $-40 < \alpha < 40°$ and $-40 < \beta < 40°$ (where α is the rotation angle about the x-axis, β is the rotation angle about the y-axis, and the z-axis is parallel to the model axis of symmetry).
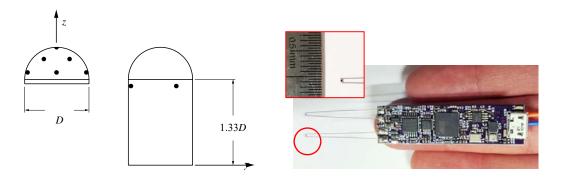

Figure 3: model configurations and sensor system and image of the sensor

RESULTS

Figure 4 shows typical profiles of the signals obtained from three of the sensors on the hemispherical model- the one on the axis, one at 40° and one at 80°. Note that a high signal indicates a high level of heat transfer. The results indicate a lower level of heat transfer from the sensor when the stagnation point is near the sensing element. The peak signal isocontour is annular, suggesting that the sensor may be responding to the geometry of the cavity in which it is fitted. The signal drops rapidly as the stagnation point moves away from the sensor and the wall shear velocity decreases. Since $L_S/D \sim 10^{-3}$ (where Ls is the length scale of the sensing element), the local response of the sensor to changes in the location of the stagnation point is expected to be reasonably independent of the model geometry; indeed, comparing the response maps of the sensors mounted on the two models demonstrated were within the range of unit-to-unit variability.
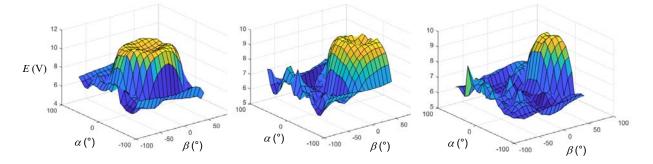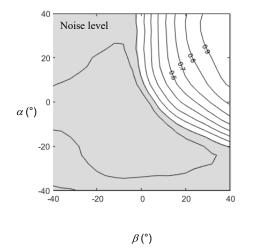

Figure 4: Signals obtained from three sensors on the hemispherical model

Individual sensors could then be calibrated for local velocity magnitude, while families of sensors could be calibrated to return magnitude and direction.

Since there are circumstances under which an instrumented model of this type might be used to obtain estimates of upstream conditions, the sensitivity of the cylindrical model (having the minimum required number of sensors to be capable of responding to flow from any incident direction) was then established. Figure 5 shows isocontours of constant (self-normalized) output signal E from a typical response map from one of the sensors on the cylindrical model, The sensor is sensitive over a limited range of incidence angles, as expected. To map the overall range of sensitivity of the cylindrical model to incident flows, the normalized magnitude of the signal gradient was mapped as a function of both α and β (see figure 6). As expected, the sensitivity is lowest when the stagnation point is located between sensors, and is also weak when directly over a sensor. A small region of low sensitivity is also evident around $(a,b) = (0,0)$; over this small range of angles, all of the sensing elements are located in a region of separated flow.
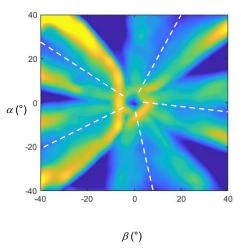

Figure 5: Isocontours of normalized signal from one of the sensors on the cylindrical model

Figure 6: Contour map of $|\nabla E|$. Dashed lines indicate sensor positions.

$$|\nabla E(\alpha, \beta)| = \sqrt{\left(\frac{\partial E}{\partial \alpha}\right)^2 + \left(\frac{\partial E}{\partial \beta}\right)^2} \qquad (1)$$

Tests were also carried out at varying free-stream temperatures T_a, in order to assess the effect of ambient temperature on the system. Over the limited range $15° < Ta < 22°$, at least, the signal response was found to vary linearly with temperature at constant speed. This suggests a reasonably simple empirical temperature correction, although this is yet to be fully developed.

CONCLUSIONS

A miniature, networkable thermal anemometry system has been developed specifically to drive CMOS-based sensing elements with negative temperature coefficients. A single, free-sensor was calibrated at speeds down to 0.5 m/s, and evidence was obtained of sensitivity down to 0.01 m/s. The sensing elements were then flush-mounted in the surfaces of two models: a hemisphere and a cylinder with a hemispherical cap. When flush-mounted, the sensor was reasonably insensitive to the external geometry if the stagnation point was located close to the sensing element. The sensors responded well to local near-surface velocities, suggesting that this technique may provide a measurable proxy for

surface pressure in model urban canopy flows, where the dimensional pressures can be too low for typical pressure transducers to resolve with sufficient accuracy. Furthermore, data from both the 13-sensor hemisphere and 5-sensor cylinder were sufficient to resolve the magnitude and direction of the incident flow, suggesting that the system may also have an application in field anemometery.

REFERENCES

Birch, D. and Martin, N. (2013) "Tracer particle momentum effects in vortex flows." J. Fluid Mech. 723, 665-691.

Fujita, H., Ohhashi, T., Asakura, M. and Watanabe, K. (1994) " A thermistor anemometer for low flow rate measurements." IEEE Trans. Instr. & Meas. 44 (3), 779-782

Mauconduit, B and Trinite, M. (1976) " New low-speed anemometer with constant temperature thermistor." J. Phys. E: Sci. Instrum. 9, 1091

Mayer, F., Haberli,A., Jacobs,H., Ofner,G., Paul,O. and Baltes,H. (1997a) "Single-chip CMOS anemometer." IEEE Tech. Digest, Int. Elec. Devices Meeting, 895–898.

Mayer, F., Paul,O., and Baltes,H. (1997b) "Flip-chip packaging for thermal CMOS anemometers." Proc. IEEE 10th Ann. Int. Workshop on MEMS, 203–208.